Structural Model of Regioregular Poly(3-hexylthiophene) Obtained by Electron Diffraction Analysis

ARTICLE *in* MACROMOLECULES · JUNE 2010

Impact Factor: 5.8 · DOI: 10.1021/ma100551m

3 AUTHORS, INCLUDING:

Navaphun Kayunkid
King Mongkut's Institute of Technology Ladk…
25 PUBLICATIONS **336** CITATIONS

Macromolecules
ARTICLE

Macromolecules **2010**, *43*, 4961–4967 **4961**
DOI: 10.1021/ma100551m

Structural Model of Regioregular Poly(3-hexylthiophene) Obtained by Electron Diffraction Analysis

Navaphun Kayunkid, Sureeporn Uttiya, and Martin Brinkmann*

Institut Charles Sadron, CNRS-Université de Strasbourg, 23 rue du Loess, 67034 Strasbourg, France

Received March 11, 2010; Revised Manuscript Received April 19, 2010

ABSTRACT: This study presents a structural analysis of regioregular poly(3-hexylthiophene) (P3HT) based on electron diffraction from epitaxied thin films. Epitaxial orientation of the hexane fraction of P3HT was performed by slow rate directional solidification in 1,3,5-trichlorobenzene leading to highly oriented and crystalline P3HT films with different contact planes. Representative electron diffraction patterns corresponding to different zone axes were obtained by the rotation-tilt electron diffraction method. A trial-and-error method based on molecular modeling and calculation of the electron diffraction patterns for the different zone axes was used to determine the crystal structure of P3HT. The unit cell is monoclinic with space group $P2_1/c$ and two chains per cell ($a = 1.60$ nm, $b = 0.78$ nm, $c = 0.78$ nm and $\gamma = 86.5$ deg). The stacking period of successive polythiophene backbones along the b axis is 0.39 nm but short interplanar distances of 0.34 nm are observed because the conjugated polythiophene backbones are tilted to the b axis. The n-hexyl side groups crystallize in an orthogonal subcell with parameters $a_s = 0.7$ nm and $b_s = 0.78$ nm. The present structural model highlights the essential role of the linear side chain crystallization on the supra-macromolecular packing of "hairy-rod" polymers like P3HT.

I. Introduction

Semiconducting polymers belong to one of the most interesting class of functional materials and are now widely used for the fabrication of electronic devices in plastic electronics.[1] Among all semiconducting polymers, regioregular poly(3-alkylthiophene)s (P3Ats) have attracted much interest as they combine facile processability and high charge carrier mobilities useful in the elaboration of organic field effect transistors (OFETs) and polymer solar cells (PSCs).[2] For both applications, structure and organization of the active layers needs to be monitored and controlled from the molecular scale to the mesoscale by controlling the crystallization of P3ATs. Various studies have evidenced the strong correlation existing between the morphology and orientation of the P3Ats in the thin films and the corresponding transport properties.[3−9] In particular, different groups have demonstrated that the macromolecular parameters of P3HT control its crystallization: the higher the average molecular weight, the lower the crystallinity in the films.[10]

Allthough P3HT is now widely used, its crystal structure has been analyzed only partly. Prosa et al. proposed the first model of P3Ats involving a lamellar structure of strongly π-conjugated polythiophene chains separated by layers of alkyl side chains.[11,12] Tashiro et al. proposed various possible structural models of P3HT and P3DT (poly(3-decylthiophene)) by using molecular modeling and X-ray diffraction on stretch-oriented films with a fiber symmetry.[13] More recently, Arosio et al. proposed a structural model of form I′ of regioregular poly(3-butylthiophene).[14] Their model was obtained from a combination of Rietveld refinement of a powder X-ray diffraction pattern and extensive molecular mechanics calculations. There has been also some attempts to derive both the structure and the electronic properties of P3HT by using first principle density-functional theory methods.[15] However, none of these studies reported single-crystal like diffraction patterns corresponding to well oriented crystalline domains of P3HT. This is largely due to the fact that, contrary to most polyolefins, it is very difficult to grow extended lamellar single crystals of P3HT. Instead, P3HT tends to form long nanofibrils in poor solvents such as cyclohexanone or anisole.[16−18] This problem can be circumvented by using selected area electron diffraction on highly oriented P3HT films grown by epitaxy.[19] As demonstrated recently in the case of poly(9,9-di-*n*-octylfluorene) and poly(9,9-bis(2-ethylhexyl)fluorene), use of selected area electron diffraction on highly oriented polymer layers opens the route to a powerfull structural refinement of these hairy-rod polymers.[20,21] Regarding the class of P3ATs, Brinkmann and Wittmann reported that highly oriented and crystalline thin films of P3ATs can be prepared by directional epitaxial crystallization in 1,3,5-trichlorobenzene. The TEM analysis of such films revealed the semicrystalline structure of various P3Ats, i.e., the periodic alternation of crystalline lamellae and amorphous interlamellar zones.[22,23] The benefits of the epitaxial orientation of polymers lies in the possibility to grow extended domains with both a well-defined contact plane on the substrate and a high *in-plane* orientation of the crystalline domains. In addition, the directional epitaxial crystallization of P3HT in TCB is particularly interesting since the substrate used for orientation, TCB, can be readily removed by evaporation under primary vacuum without altering the crystalline structure of the P3HT films. Accordingly, it is possible to obtain electron diffraction patterns of highly oriented and crystalline thin films of P3HT without any contribution from the substrate. In other words, an epitaxied sample composed of multiple lamellar domains can provide "single-crystal"-like electron diffraction patterns in contrast to the rather complex X-ray diffraction patterns obtained with oriented fibers or polycrystalline powders. In the case of low molecular weight P3HT (M_w = 7.3 kDa), it was possible to identify a monoclinic unit cell with parameters $a = 1.6$ nm, $b = 0.78$ nm, $c = 0.78$ nm, and $\gamma = 93.5$ deg from the single-crystal like electron diffraction pattern corresponding to the [0 0 1] zone.[10] Herein, we describe a structural

*Corresponding author. E-mail: brinkman@ics.u-strasbg.fr.

Published on Web 05/07/2010

Table 1. Macromolecular SEC Parameters (M_n, M_w and PDI = M_w/M_n) for the P3HT Samples[a]

sample	M_n (kg/mol equiv of PS)	M_w (kg/mol equiv of PS)	PDI
P3HT as-received	13.11	17.16	1.31
P3HT hexane fraction	7.27	7.86	1.08

[a] A dn/dc value of 0.259 ± 0.026 mL/g was measured for the as-received sample.

refinement of P3HT using electron diffraction on highly oriented P3HT samples grown by a slow rate directional crystallization method. The experimental procedure yield a set of 44 independent reflections and 4 distinct projections in reciprocal space. The refined structural model highlights the essential role of the *n*-hexyl side-chains on the crystallization behavior of "hairy-rod"-like polymers.

II. Experimental Section

P3HT was purchased from Merck and fractionated by Soxhlet extraction in *n*-hexane. The P3HT samples were characterized by multiple detector size exclusion chromatography (SEC) using THF (HPLC grade) as the eluent and a PS calibration. The SEC setup consisted of a Shimadzu LC10AD pump, an ERMA ERC3512 online degasser, a WATERS 717+ automatic injector and five 300 × 7.5 mm^2 PL Gel columns from Polymer Laboratories (4 × 10 mm Mixed-B and one 500 Å) connected in series and a refractive index (RI) detector (Shimadzu RID10A). The macromolecular parameters obtained by SEC (polystyrene standard) are collected in Table 1. The hexane fraction of the P3HT sample used herein is characterized $M_w = 7.9$ kDa which is very similar to the sample used in our previous study, but it shows a very low polydispersity index (PDI) of 1.08.

1. Epitaxied thin films were prepared by using a slight modification of the directional epitaxial crystallization method in 1,3,5-trichlorobenzene (TCB) described in ref 10. In brief, the principle of this method consists in using a crystallizable solvent playing successively the role of (i) the solvent for P3HT in its liquid form and (ii) once crystallized the substrate for the epitaxial crystallization of the polymer. The method used in this work has been substantially improved by controlling the growth rate of the TCB crystal. Rather than moving manually the sample consisting of a P3HT-TCB solution between two glass slides at ca. 1−2 mm/s on a Koeffler bench, we used a motorized translation bench allowing for a constant 0.2 mm/s translation speed of the sample from the hot zone (hot bar maintained at a constant temperature of 75 °C) to the cold zone kept at room temperature. In this manner, the crystallization front of the TCB advances at a constant and reproducible speed. Uniform and large areas of highly oriented TCB substrates suitable for the epitaxial growth of highly oriented P3HT are consistently obtained (Figure S1). The morphology of oriented TCB films grown by both methods is displayed in Figure S1 of the Supporting Information. The TCB was slowly evaporated at room temperature in a primary vacuum (10^{-2}mbar) for 1 h to recover the extended stripes of the oriented P3HT of interest (see Figure 1). Highly oriented areas were subsequently selected by optical microscopy (Leica DMR-X microscope). The P3HT films were coated with a thin amorphous carbon film and the P3HT/carbon film was removed from the glass substrate by using the "polyacrylic acid" method and subsequently recovered onto TEM copper grids. TEM was performed in both bright field and diffraction modes using a Philips CM12 microscope equipped with a MVIII CCD camera (Soft Imaging System). The acquisition conditions for the electron diffraction (ED) patterns are as follows. First, in bright field mode, the electron beam is spread on the fluorescent screen until no light can be detected by the bare eye. Under these illumination conditions, the typical ED pattern can be recorded on the CCD camera with an exposure time in the range 1−5 s. The overall lifetime of the ED pattern does not exceed 10−30s. Beam damage is mainly manifested by the fading of the (h 0 0) reflections. Image treatment was performed by using the AnalySIS software (Soft Imaging System). Molecular modeling was performed on a Silicon Graphic station using the Cerius2 program. A trial-and-error procedure was used to refine the crystal structure of P3HT, following the same methodology as used previously to refine the crystal structures of poly(9,9-di-*n*-octyl-fluorene) and poly(3-hydroxy-*p*-methylphenylvalerate).[21,24] For each step of the trial-and-error method, the molecular geometry was optimized using the "clean" procedure of the Cerius2 Program (additional informations on this procedure are avaible in the user's guide on the modeling environment).

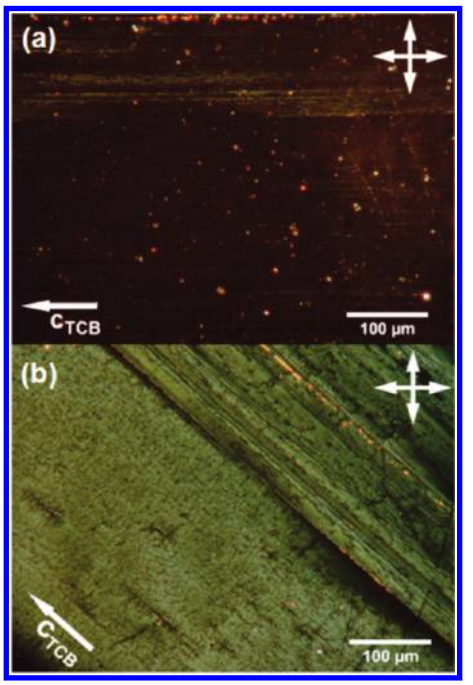

Figure 1. Highly oriented area of a P3HT thin film grown by the slow-rate directional epitaxial crystallization method as observed under the polarized optical microscope with crossed polarizers: (a) P3HT chain axis oriented parallel to the polarizer and (b) at 45° to the polarizer.

III. Results and Discussion

1. Various Contact Planes on the TCB Substrate. In our previous study on epitaxially oriented low-M_w P3HT, we could clearly identify both flat-on and edge-on oriented crystallines lamellae of P3HT corresponding to (0 0 1) and (0 1 0) contact planes on the TCB substrate.[10] These two type of domains were also identified by high resolution transmission electron microscopy.[23] The edge-on oriented lamellae give rise to the typical ED pattern shown in Figure 2a. Remarkably, it displays very sharp h 0 0 reflections up to the seventh order on the equator. Along the meridian, i.e., the chain axis direction, note the absence of the 0 0 4 reflection but the presence of a weak 0 0 6 reflection (see the section profile plot along the meridian shown in Figure S2 of the Supporting Information). The first layer line shows the characteristic 0 0 2, 1 0 2, 2 0 2, and 5 0 2 reflections. With respect to our earlier work, the better control of the TCB growth front achieved by the use of a "slow" growth rate explains the better definition of the ED pattern.

Additional orientations of the P3HT lamellae, not observed in our previous work,[10] were obtained, as illustrated by original ED patterns shown in parts b and c of Figure 2.

The equatorial reflections in Figure 2.b are indexed as (h 0 0) with $h = 1$, 2, and 3. The corresponding reflections on the first layer line at 0.52, 0.46, and 0.39 nm (see Table 2) are

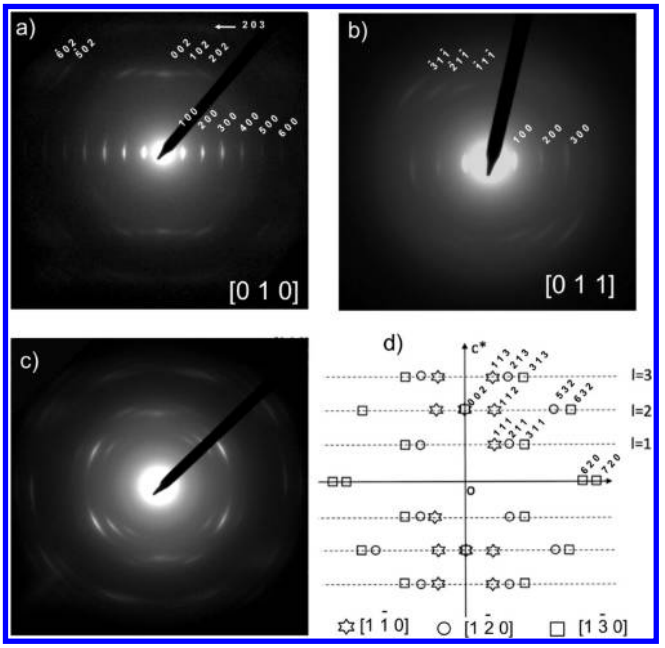

Figure 2. Various electron diffraction patterns of an epitaxied thin film of P3HT corresponding to different zone axes: (a) [0 1 0] zone, (b) [0 1 1] zone. Note the asymmetry of the intensity of the $(-h\ 1\ -1)$ reflections (h = 1, 2, 3). (c) This pattern is the superposition of ED patterns corresponding to [1 −1 0], [1 −2 0] and [1 −3 0] zones as illustrated in part d). The reflections arising from three nearby zones are identified by different symbols.

Table 2. Orientation Parameters of the Backbone and the 3-Hexyl Side Chain with Respect to the Unit Cell Axes (See Figure 6)

method	θ_1 (deg)	θ_2 (deg)	θ_3 (deg)	θ_4 (deg)
XRD and modeling[a]	33	52		
DFT calculations[b]	6.9	39.2	34	
this work	26 ± 5	−29 ± 5	0 ± 1	90 ± 3

[a] These values are deduced from the structural model 3 given in ref 13. [b] Ref 15.

consistently indexed by using the unit cell parameters of the monoclinic cell as −1 1 −1, −2 1 −1, and −3 1 −1 respectively.[10] Accordingly, the ED pattern in Figure 2b is characteristic of the [0 1 1] zone and arises from crystalline P3HT lamellae with a (0 1 1) contact plane on the TCB substrate.

Figure 2c shows another characteristic ED pattern. The main reflections on the first layer line are indexed as (h 1 1) with h=1, 2, and 3. Allthough these reflections correspond to different zones, they are observed simultaneously for two main reasons. First, the reflections in Figure 2.c are strongly arced, suggesting a rather broad distribution of domain misorientation. Since, the angle between [1 −2 0] and [1 −3 0] zones is only 11°, crystalline domains with slightly different orientations to the incident electron beam can give rise to the ED of either [1 −2 0] or [1 −3 0] zones.[25] Second, the reduced thickness of the crystalline domains in the direction parallel to the incident electron beam can cause the reflections to be elongated in this direction. Accordingly, the reflection corresponding to different close lying zones can intersect the Ewald sphere and contribute to the overall ED pattern in Figure 2c. As shown hereafter, this ED pattern arises from tilted P3HT lamellae such that the *n*-hexyl side chains are oriented almost perpendicular to the TCB substrate (see section III.3).

We assume that the additional orientations of the P3HT lamellae on the TCB substrate identified above are possibly due to the combination of both (i) the low M_w and polydispersity of the P3HT sample and (ii) the better control of the growth kinetics of the TCB crystals by using a slow and controlled growth rate. The low M_w and polydispersity of the P3HT fraction should ease the crystallization of extended P3HT chains in the form of lamellar domains without chain folding. Additional experiments to investigate the impact of TCB growth rate on the orientation of P3HT are currently in progress.

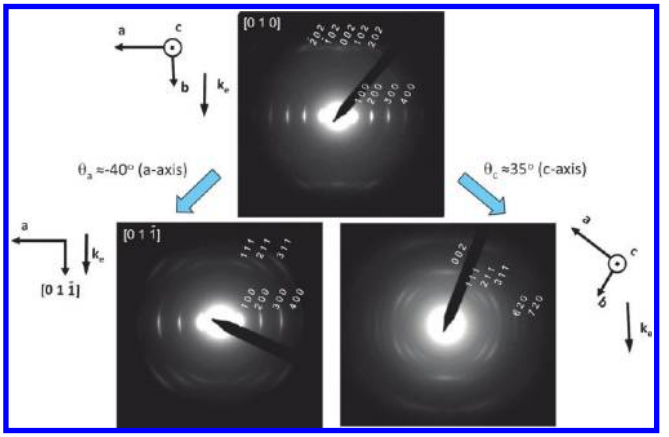

Figure 3. Rotation-tilt experiment performed on an oriented P3HT film (7.9 kDa) grown by slow-rate directional crystallization in TCB. The sample shows initially a (0 1 0) contact plane ([0 1 0] zone). A tilt around the *a* axis by ∼40° yields the ED pattern typical of the [0 1 −1] zone with some contribution from the [0 1 1] zone. A tilt of the sample around the *c* axis by 35° yields an ED pattern corresponding to the superposition of the [−1 k 0] zones with k = 1, 2, and 3.

2. Rotation-Tilt Experiments. Extended areas (several hundreds of μm^2) of P3HT films with uniform *in-plane* orientation and a well-defined contact plane are very usefull to investigate in more details the structure of P3HT by rotation-tilt ED experiments. Tilting the sample around identified crystallographic directions in the TEM yields different sections of the reciprocal space which can be used to further refine the crystal structure of the polymer. It is in particular useful to identify the reflection rules, i.e., the space group of the crystal structure.

Figure 3. depicts the result of a first rotation-tilt experiment on a P3HT sample with (0 1 0) contact plane. The tilt of the sample around the *a* axis by $\theta_a \sim -40°$ yields an ED pattern which is typical of the [0 1 −1] zone. It is worth noting that the same ED patterns are obtained by titlting the sample at $+\theta_a$ or $-\theta_a$ around the *a* axis. This is quite different if the sample is tilted around the *c* axis. When $\theta_c \sim 35°$, a pattern almost identical to that of Figure 2.c is obtained, which corresponds to the overlap of the contributions from the [1 −2 0], and the [1 −3 0] zones. As seen in Figure 4, for $\theta_c = -40°$, the ED pattern is clearly distinct from that observed for $\theta_c = +40°$. As shown hereafter, the two tilts correspond to two specific orientations of the electron beam with respect to the P3HT chains, namely parallel and perpendicular to the *n*-hexyl side chains (see insets in Figure 4).

Figure 5 illustrates the second rotation-tilt experiments on a P3HT sample area showing a typical (0 1 1) contact plane. This contact plane is interesting because, as shown in the insets of Figure 5, a tilt by ∼ +45° around the *a* axis gives rise to the [0 0 −1] zone whereas a tilt by ∼ −45° yields a pattern corresponding to the [0 −1 0] zone. Indeed, as expected from our previous work,[10] the ED pattern of the [0 0 −1] zone shows the h 0 0 equatorial reflections (h=1, 2, 3) and the typical h 2 0 (h=0, 1, 2, 3) reflections on the first layer line.

3. Determination of the Space Group and Structural Refinement. As demonstrated recently in the case of PFO and

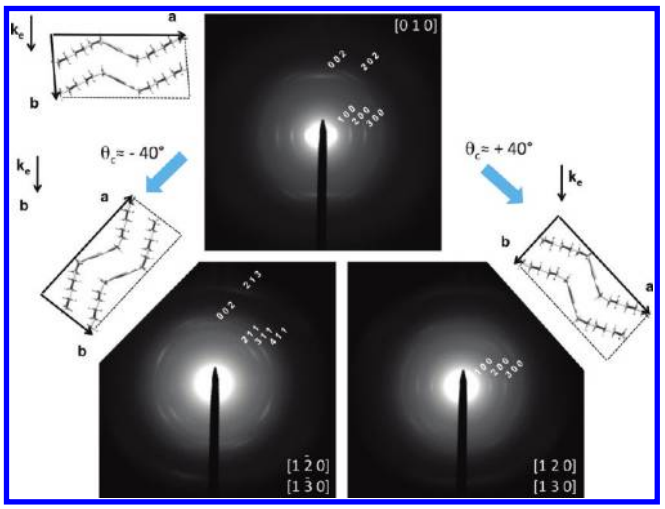

Figure 4. Rotation-tilt experiments on an oriented thin film of P3HT (7.9 kDa) grown by slow-rate directional crystallization in TCB and showing a (0 1 0) orientation. For a $\theta_c \sim 40°$ tilt around the *c* axis, the electron beam (k_e) is approximately parallel to the *n*-hexyl side chains (see the insets). For $\theta_c \sim -40°$, k_e is almost perpendicular to the side chains. Note the quasi absence of reflections on the $l = \pm 1$ layer lines.

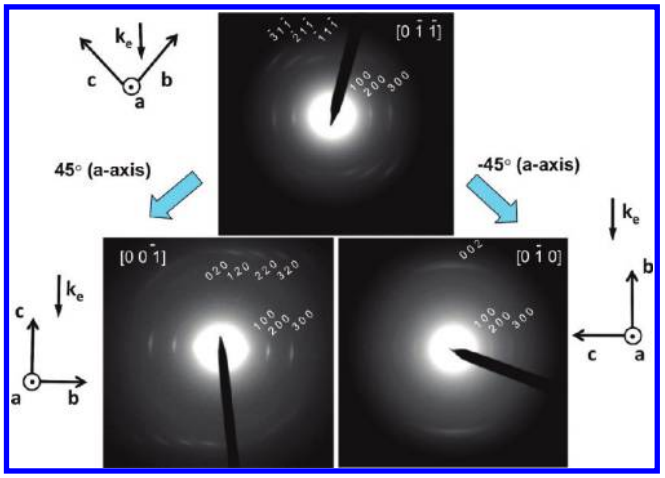

Figure 5. Rotation-tilt experiment performed on an oriented P3HT film grown by slow-rate directional crystallization. The ED pattern from the nontilted sample corresponds to the [0 −1 −1] zone. The ED pattern of the [0 0 −1] zone is obtained by a tilt of $\theta_a = 45°$ around the *a* axis whereas a tilt of $\theta_a = -45°$ yields a pattern corresponding to the [0 −1 0] zone. The insets show the relative orientation of the unit cell and the incident electron beam with scattering vector k_e.

PF2/6, the possibility to record numerous diffraction patterns corresponding to different zone axes allows to identify the reflection rules and determine the space group of the crystal structure. The observed reflection rules are:

$$00l, \text{ with } l = 2n \ (n \text{ is an integer}) \quad (1)$$

$$0k0, \text{ with } k = 2n \quad (2)$$

and

$$(h\,k\,0) \text{ with } k = 2n \quad (3)$$

They are compatible with a $P2_1/c$ space group with unique axis *c*.[26] This space group has also been considered in the recent study by Arosio et al. on form I′ of poly(3-butylthiophene).[14] With this space group and the determined cell

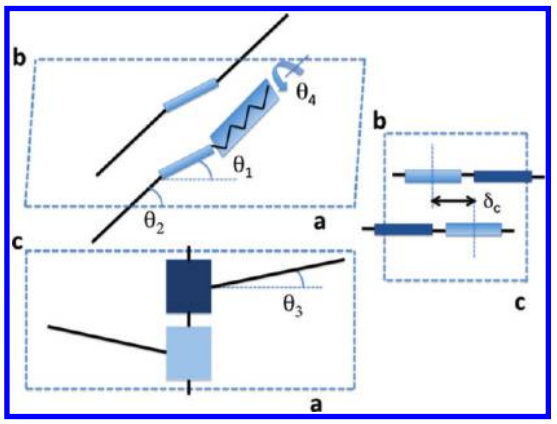

Figure 6. Schematic drawing of the P3HT structural model defining the angles θ_1, θ_2, θ_3, and θ_4 used for the structural refinement. $\theta_4 = 0°$ when the plane containing the *all-trans* zigzag of the *n*-hexyl chain is oriented parallel to the (*a*, *b*) plane.

parameters, we need to define the atomic coordinates of one monomeric unit only, all three others being symmetry-related to it. To construct a molecular model of the polythiophene backbone, we used the atomic coordinates reported for α-sexithiophene (α-6T).[27,28] *n*-hexyl side-chain with an *all-trans* conformation was "attached" to the thiophene monomer in the position 3. The *all-trans* planar zigzag conformation has been established by Tashiro et al. using FTIR spectroscopy.[29] The position of the 3-hexylthiophene monomer in the cell was refined so as to obtain a correct polythiophene backbone conformation with a thiophene−thiophene bond length of 0.145 nm and proper bond angles as observed for instance in α-6T.[27,28]

In a second step of the structure determination, the polymer backbone and the side-chain orientations in the unit cell were determined. To this aim, we used rotational angles labeled θ_1, θ_2, θ_3, and θ_4 as defined in Figure 6. For a given geometry of the monomer, we calculated the ED patterns for the three zone axes [0 1 0], [0 0 1] and [0 1 1], i.e., for the most representative experimental ED patterns. The structural model was progressively improved by trial-and-error so as to yield the best agreement between the three calculated and experimental ED patterns. It must be emphasized that, contrary to the direct methods based on quantitative intensity data, the present approach is based on a qualitative comparison of the peak intensities.[30] Nevertheless, this qualitative aspect is counterbalanced by the fact that the best possible agreement between calculated and experimental patterns must be reached for a set of three different zone axes. The main guidelines and steps used in the present process are as follows.

A remarkable feature of the [0 0 1] zone ED pattern is the asymmetric intensity of the reflections on the first and second layer lines (see Figure 7 in ref 10). This asymmetry is essentially determined by the θ_1 and θ_2 angular orientations of the backbone and the side chains in the (*a*, *b*) plane. Moreover, this asymmetry is not compatible with the side-chains pointing alternatively up and down in successive layers along the *a* axis, as proposed by Prosa et al.[11] As a matter of fact, two combinations of (θ_1, θ_2) allow to reproduce the asymmetry of the [0 0 1] pattern namely (16°, 44°) and (−25°, 29°). However, in the former case, the intensity sequence of the h 0 0 reflections does not fit the experimental data (the calculated intensity I_{200} is clearly underrated as seen in Figure S3). In the latter case, a very good agreement between calculated and experimental ED patterns for this [0 0 1] zone is obtained i.e. $\theta_1 = -26 \pm 5°$ and $\theta_2 = 29 \pm 5°$.

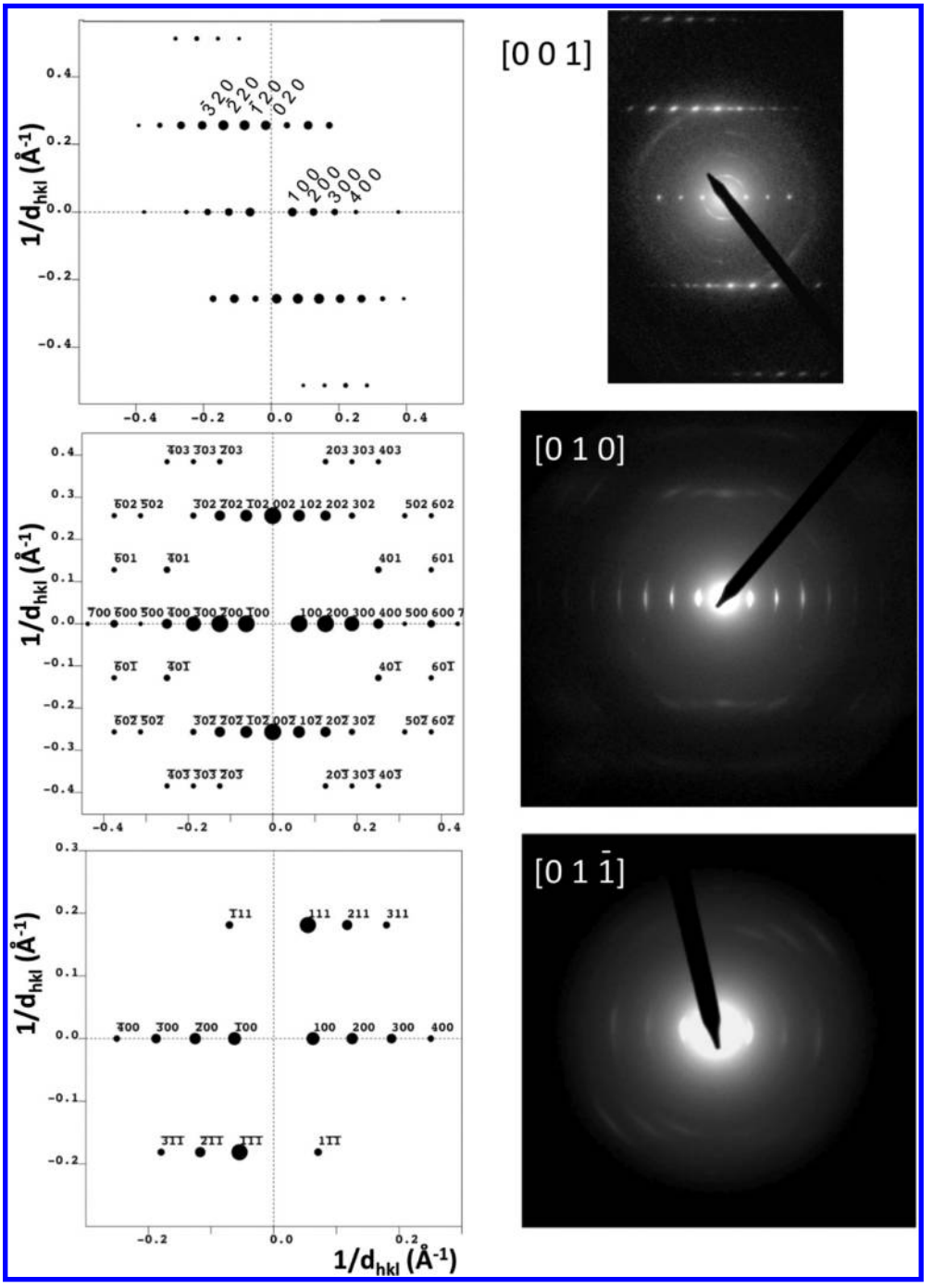

Figure 7. Calculated (left) and experimental (right) electron diffraction patterns corresponding to the determined crystal structure of P3HT for three different zone axes. The presence of additional reflections on the first layer line of the [0 0 1] zone is related to a twinning within the crystalline P3HT lamellae (the (b,c) plane is the twinning plane).[10]

When determining the orientation of the *all-trans n*-hexyl side chain in the (*a*, *c*) plane, the intensities of the reflections in the [0 1 0] zone ED pattern are most useful. The absent 0 0 4 and the weak 0 0 6 reflections as well as the extinction of the (*h* 0 1) reflections with $h = 1, 2, 3$ (see Figures 2 and S2) are most characteristic. These features depend on three main parameters: (i) the relative shift δ_c along the *c* axis between the two chains (see Figure 6), (ii) the orientation of the planar zigzag conformation of the hexyl group relative to the (*a*, *c*) plane (θ_4 angle) and (iii) the θ_3 angle, i.e., the projected direction of the side chain in the (*a*, *c*) plane.

The quasi-absence of all (*h* 0 1) reflections (except for a weak 4 0 1) is only possible if $\theta_3 = 0°$ i.e. the hexyl side chains are oriented perpendicular to the polythiophene backbone. In Figure S4 of the Supporting Information, we depict the calculated ED pattern when θ_3 is set to a value of 3°. Additional 1 0 1 and 2 0 1 reflections appear in the ED pattern of the [0 1 0] zone. The fact that $\theta_3 = 0°$ is clearly different from the strutural model of P3HT of Maillard and Rochefort ($\theta_3 = 34°$) and of the model of form I′ of regioregular poly(3-butylthiophene) (P3BT) by Arosio et al.[15,14] These structural models were based on DFT calculations and a combination of Rietveld refinement of a X-ray powder pattern combined with molecular mechanics calculations, respectively.

Once, the side chain orientation is defined, one needs to define the orientation of the plane containing the *n*-hexyl side

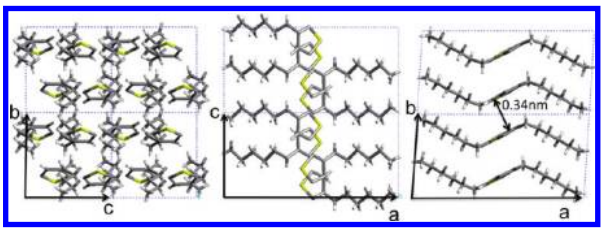

Figure 8. Projections of the P3HT crystal structure along the *a*, *b*, and *c* axes of the unit cell.

chain with the *all-trans* conformation, i.e., the θ_4 angle. A critical test is the weakness or even the absence of the 0 0 4 reflection (see Figure S2). If the plane of the *n*-hexyl chain is set perfectly parallel to the (*a*, *b*) plane ($\theta_4 = 0°$), the calculated 0 0 4 reflection is relatively strong whatever the relative shift δ_c between the two chains in the cell. Actually, there is only one peculiar combination of the relative shift δ_c and θ_4 for which the 0 0 4 is absent and a weak 0 0 6 is present.

The calculated ED patterns for the crystal structure of P3HT determined by these means are compared with the experimental patterns in Figure 7. For all zone axes, the agreement between the intensities of the most intense reflections in the calculated and experimental patterns is good. In particular, the intensities of the *h* 0 0 reflections follow the sequence $I_{100} > I_{200} > I_{300} > I_{400}$ (see Figure 7a). Moreover, the calculated ED pattern for the [0 0 1] zone reproduces well the asymmetry of the principal reflections of the first and second layer lines and the relative intensities of the *h* 0 0 reflections with respect to the *h* 2 0 reflections is also respected. Similarly, the calculated fiber pattern, shown in Figure S5 of the Supporting Information, compares well with the ED pattern obtained for oriented P3HT with M_w = 18 kDa.[13,22] Some discrepancies are however observed between calculated and experimental patterns. The experimental [0 1 0] ED pattern in Figure 7 shows that the 0 0 2 reflection is not as sharp as the h 0 0 reflections and that the observed intensity of this reflection is not as high as in the calculated pattern. In our previous HR-TEM study, we have shown that the size of the crystalline domains in the direction parallel to the chains is approximately 7 nm whereas in the direction of the *a* axis, the crystalline domains extend over 50−100 nm.[23] The calculated ED pattern do not take into account this in-plane anisotropy of the crystal size but only the thickness of the diffracting domains. Accordingly, one possible explanation for the low intensity of the observed 0 0 2 reflection could be the limited size of the crystalline domains along the *c* axis direction. One additional origin for the week 0 0 2 could be the presence of structural disorder along the chain axis direction as induced for instance by regioregularity defects.

4. Major Features of the P3HT Crystal Structure. The projections of the P3HT crystal structure as seen along the *a*, *b*, and *c* axes of the unit cell are shown in Figure 8. The present model bears some similarity with the model 3 of Tashiro et al.[13] (except for the unit cell parameters) and with the structure proposed by Maillard and Rochefort[15] (see Table 2). There are however significant differences.[15] The structure by Maillard and Rochefort predicts a π-stacking distance of 0.342 nm that is shorter than the repeat period of the P3HT chains along the *b* axis which amounts to 0.39 nm.[13,12] In the present structural model, the stacking distance of polythiophene backbones is also equal to 0.39 nm (*b*/2) which is much larger than the interplanar distance of 0.34 nm obtained from DFT calculations.[15] A simple way to reconcile both these values is to tilt the conjugated backbones (θ_1 angle) with respect to the stacking axis (*b* axis) similarly to

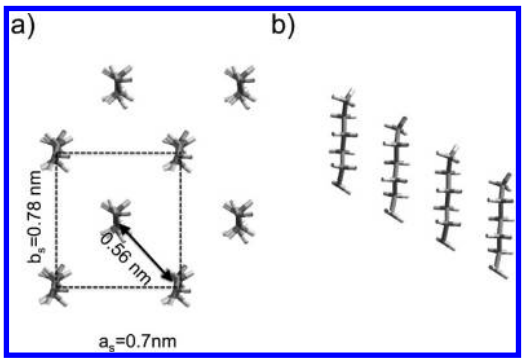

Figure 9. Rectangular subcell accounting for the packing of the *n*-hexyl side chains in the crystal structure of P3HT. (a) projection along the *n*-hexyl side chain direction (corresponding to the direction [1 2 0] in the unit cell of P3HT) and (b) projection along the b_s axis of the orthogonal subcell.

what is observed in the columnar stacks of phthalocyanine molecules.[25] As seen in Figure 8, a 26° tilt of the polythiophene conjugated backbone to the *b* axis leads to a rather short interplanar distance of approximately 0.34 nm and leads to a good agreement of the calculated and experimental ED patterns for the [0 0 1] zone.[15] In this manner the present structural model reconciles the stacking period of $b/2 = 0.39$ nm along the *b* axis and the existence of a short interplanar π-stacking of the polythiophene backbones as predicted by the DFT calculations of Maillard and Rochefort.[15]

A further important difference with the model of Maillard and Rochefort deals with the relative shift δ_c between two chains in the unit cell along the *c* axis (see Figure 6). In their model, δ_c is set equal to a multiple of *b*/2. The structural evidence gathered in this study, especially the intensity distribution of the 0 0 1 reflections indicates clearly a different relative shift between the two P3HT chains in the unit cell along the *c* axis. The same holds true for the crystal structure of form I′ of P3BT proposed by Arosio et al.[14]

The packing of the *n*-hexyl side chains in the structure of P3HT is particularly interesting. Figure 9 displays the projections of the *n*-hexyl side chain along the chain axis and along a direction perpendicular to it. Overall, the *n*-hexyl side chains are separated by a distance of ∼0.56 nm, which is larger than the expected distance between polyethylene chains (∼0.435 nm).[31] These *n*-hexyl side are actually arranged in a centered rectangular subcell with parameters a_s = 0.7 nm and b_s = 0.78 nm, yielding a cross-sectional area per chain of ∼0.27 nm^2. This subcell happens to be substantially larger than the $O_\perp$ subcell proposed by Kitaigorodsky (a_s = 0.743 nm and b_s = 0.501 nm).[31] However, in the present case, the plane of the *n*-hexyl zigzag is oriented parallel to b_s axis whereas in the $O_\perp$ cell, it is tilted to this direction, allowing for a denser packing. Moreover, it should be kept in mind that the short *n*-hexyl side chains are fixed at one of their ends on the polythiophene backbone. In spite of this conformational restriction, they are able to adopt an orientation in the cell that results in a relatively ordered packing, not a disordered one as proposed by Kline et al.[32] This peculiar side-chain packing was not possible in the models of Arioso et al. on form I′ of P3BT since the butyl side chains are not oriented perpendicular to the polythiophene backbone.[14,15] In the structural model of form I′ of P3BT, the butyl side chains are too short to allow for a regular packing whereas the longer *n*-dodecyl side chains are reported to be interdigitated.[13]

It would be very interesting to analyze whether the peculiar π-stacking of the polythiophene backbones in P3HT is

dictated by the crystallization of the *n*-hexyl side chains or, if it is the π-stacking of the polythiophene backbone that enforces the stacking of the *n*-hexyl side chains. It seems that the shift δ_c between the conjugated backbones of the successive P3HT chains is determined to some extent by the packing of the *n*-hexyl side chains in the direction of the *a* axis. This situation reminds that encountered previously in the case of PFO for which the linear *n*-octyl side chains crystallize in a rather specific manner, forcing the polyfluorene backbone to adopt a more or less planar conformation.[23]

There is another remarkable characteristic of the P3HT structure refined herein, namely the fact that, contrary to the previous studies, the *n*-hexyl side-chains are oriented in a plane perpendicular to the conjugated polythiophene backbone ($\theta_3 = 0°$). This structure bears an intrinsic advantage with respect to chain folding. As reported by Arosio et al., if $\theta_3 \neq 0°$, it is necessary to distinguish so-called "up" and "down" chains in the crystal (see Figure 8 in ref 14). This implies that folding P3HT chains cannot re-enter a lamellar crystal at any position and, hence, restricts the fold structure, contrary to the situation observed for our structural model of P3HT.

4. Conclusion

A structural model of P3HT has been determined by electron diffraction and rotation-tilt experiments on highly oriented P3HT films grown by a slow rate directional epitaxial crystallization method. For relatively low M_w P3HT, this growth method generates extended oriented areas with different contact planes including edge-on and inclined crystalline lamellae. The structural model underlines the importance of the *n*-hexyl side chains in the crystallization of P3HT as well as the existence of short π-stacking distances (0.34 nm) between successive polythiophene backbones. The crystal packing in P3HT is not only determined by the strong π-stacking interactions along the *b* axis but also by the *n*-hexyl side chains crystallizing in a rectangular subcell. From the methodology standpoint, this work illustrates the possibility to investigate the structure of a complex conjugated polymer like P3HT by using the qualitative analysis of various ED patterns corresponding to well-defined zones, combined with molecular modeling. This starting model might further be improved by using so-called "direct methods" based on the quantitative analysis of intensity data.

Acknowledgment. Enlighting discussions with Dr Bernard Lotz are gratefully acknowledged. We are also gratefull to Catherine Foussat and Alain Rameau for performing the SEC measurements. Financial support by the French Ministry of Foreign Affairs through a Hubert Curien project (Nanostructured Interfaces in Electroactive Organic Architectures) is gratefully acknowledged. Additional financial support was provided by the Agence Nationale de la Recherche under Contract ANR-08-NANO-012-01. This work is dedicated to Christine Straupé who just passed away, in memory of her contribution to the study of polymer crystallization.

Supporting Information Available: Figures showing oriented TCB film grown by slow-rate directional crystallization method and experimental and calculated electron diffraction patterns and tables giving a list of the reflections and the atomic coordinates. This material is available free of charge via the Internet at http://pubs.acs.org.

References and Notes

(1) Salleo, A. *Mater. Today* **2007**, *10*, 38–45.
(2) Sirringhaus, H.; Brown, P. J.; Friend, R. H.; Nielsen, M. M.; Bechgaard, K.; Langeveld-Voss, B. M. W.; Spiering, A. J. H.; Janssen, R. A. J.; Meijer, E. W.; Herwig, P.; de Leeuw, D. M. *Nature* **1999**, *401*, 685–688.
(3) Kline, R. J.; McGehee, M. D.; Kadnikova, E. N.; Liu, J.; Fréchet, J. M. J.; Toney, M. F. *Macromolecules* **2005**, *38*, 3312–3319.
(4) Verilhac, J. M.; LeBlevennec, G.; Djurado, D.; Rieutord, F.; Chouiki, M.; Travers, J.-P.; Pron, A. *Synth. Met.* **2006**, *156*, 815–823.
(5) Bao, Z.; Dodabalapur, A.; Lovinger, A. *Appl. Phys. Lett.* **1996**, *69*, 4108.
(6) Zhang, R.; Li, B.; Iovu, M. C.; Jefferies-EL, M.; Sauvé, G.; Cooper, J.; Jia, S.; Tristram-Nagle, S.; Smilgies, D. L.; Lambeth, D. N.; McCullough, R. D.; Kowalewsky, T. *J. Am. Chem. Soc.* **2006**, *128*, 3480–3481.
(7) Zen, A.; Saphiannikova, M.; Neher, D.; Grenzer, J.; Grigorian, S.; Pietsch, U.; Asawapirom, U.; Janietz, S.; Scherf, U.; Lieberwirth, I.; Wegner, G. *Macromolecules* **2006**, *39*, 2162–2171.
(8) Kline, R. E.; McGehee, M. D.; Kadnikova, E. N.; Liu, J.; Fréchet, J. M.; Toney, M. F. *Adv. Mater.* **2003**, *15*, 1519–1522.
(9) Yang, H.; Shine, T. J.; Yang, L.; Cho, K.; Ryu, C. Y.; Bao, Z. *Adv. Funct. Mat.* **2005**, *15*, 671–676.
(10) Brinkmann, M.; Rannou, P. *Adv. Funct. Mater.* **2007**, *17*, 101–108.
(11) Prosa, T. J.; Winokur, M. J.; Moulton, J.; Smith, P.; Heeger, A. J. *Macromolecules* **1992**, *25*, 4364.
(12) Prosa, T. J.; Winokur, M. J.; McCullough, R. D. *Macromolecules* **1996**, *29*, 3654.
(13) Tashiro, K.; Kobayashi, M.; Kawai, T.; Yoshino, K. *Polymer* **1997**, *38*, 2867.
(14) Arosio, P.; Moreno, M.; Famulari, A.; Raos, G.; Catellani, M.; Meille, V. S. *Chem. Mater.* **2009**, *21*, 78.
(15) Maillard, A.; Rochefort, A. *Phys. Rev. B* **2009**, *79*, 115207.
(16) Ihn, K. J.; Moulton, J.; Smith, P. *J. Polym. Sci., Polym. Phys.* **1993**, *31*, 735–742.
(17) S. Berson, S.; De Bettignies, R.; Bailly, S.; Guillerez, S. A. *Adv. Funct. Mater.* **2007**, *17*, 1377.
(18) Samitsu, S.; Shimomura, T.; Heike, S.; Hashizume, T.; Ito, K. *Macromolecules* **2008**, *41*, 8000.
(19) Brinkmann, M. *L'act. chim.* **2009**, *326*, 31.
(20) Brinkmann, M. *Macromolecules* **2007**, *40*, 7532.
(21) Brinkmann, M.; Charoenthai, N.; Traiphol, R.; Piyakulawat, P.; Wlosnewski, J.; Asawapirom, U. *Macromolecules* **2009**, *42*, 8298.
(22) Brinkmann, M.; Wittmann, J.-C. *Adv. Mater.* **2006**, *18*, 860.
(23) Brinkmann, M.; Rannou, P. *Macromolecules* **2009**, *42*, 1125.
(24) Hany, R.; Brinkmann, M.; Hartmann, R.; Pletscher, E.; Rentsch, D.; Zinn, M. *Macromolecules* **2009**, *42*, 6322.
(25) Kobayashi, T. In *Crystals: growth, properties and applications*: Karl, N., Ed.; Springer Verlag: Berlin, 1991; pp 2−63.
(26) *International tables of crystallography*; Hahn, T., Ed. Kluwer Academic Publishers: Dordrecht, The Netherlands, 1989, Vol. *A*, pp 199−255.
(27) Porzio, W.; Destri, S.; Mascherpa, M.; Rissini, S.; Bruckner, S. *Synth. Met.* **1993**, *55*, 408.
(28) Horowitz, G.; Bachet, B.; Yassar, A.; Lang, P.; Demanze, F.; Fave, J.-L.; Garnier, F. *Chem. Mater.* **1995**, *7*, 1337.
(29) Tashiro, K.; Ono, K.; Minagawa, Y.; Kobayashi, M.; Kawai, T.; Yoshino, K. *J. Polym. Sci., Part B: Polym. Phys.* **1991**, *29*, 1223.
(30) Tashiro, K.; Kamae, T.; Asanaga, H.; Oikawa, T. *Macromolecules* **2004**, *37*, 826.
(31) Dorset, L. D. In *Crystallography of the polymethylene chain: an inquiry into the structure of waxes, IUCr Monographs on crystallography no. 17*: Oxford University Press: New York, 2005; pp 19−28.
(32) Kline, R. J.; DeLongchamp, D. M.; Fisher, D. A.; Lin, E. K.; Richter, L. J.; Chabinyc, M. L.; Toney, M. F.; Heeney, M.; McCulloch, I. *Macromolecules* **2007**, *40*, 7960.